1. INTRODUCTION AND EXPLANATORY NOTES

Shipboard Scientific Parties[1]

BACKGROUND AND OBJECTIVES

Prior to Legs 51, 52, and 53 of the Deep Sea Drilling Project, four legs in the Atlantic Ocean (Legs 37, 45, 46, and 49) had been devoted primarily to basement drilling (Aumento, Melson et al., 1977; Melson, Rabinowitz et al., 1979; Dmitriev, Heirtzler, et al., 1979; Cann, Luyendyk, et al., 1979). The main objective of these legs, except for Leg 49, was to drill a deep hole in the oceanic crust in order to sample Layer 2 and, if possible, the upper levels of Layer 3. Although basement drilling in the Atlantic Ocean thus far has clearly established the basic composition and extrusive origin of at least the upper third of Layer 2, many important questions remain to be answered:

1) How does Layer 2 vary with depth? From the results of earlier legs, it is clear that the upper portion of Layer 2 (Layer 2A) consists largely of extrusive basalts containing a relatively large proportion of intercalated breccias, water-filled voids, and sediments having low seismic velocities. Since only the uppermost half-kilometer of Layer 2 was sampled on these legs, the constitution of the lower levels of the crust remains unknown. Is Layer 2B basically the same as Layer 2A but with a smaller proportion of low-velocity material, or does it contain a higher proportion of dikes and sills?

2) What is the nature of Layer 3? Does the boundary between Layers 2 and 3 represent a transition between massive basalt and gabbro, a metamorphic front, or a morphologic boundary between pillow basalts and massive basalts or dikes?

3) How is the oceanic crust constructed? The crust is thought to grow by extrusion and intrusion at accreting plate margins, but how long does the process take and is it continuous or episodic?

---

[1]Leg 51: Thomas W. Donnelly (Co-Chief Scientist), State University of New York, Department of Geology, Binghamton, New York; Jean Francheteau (Co-Chief Scientist), Centre Océanologique de Bretagne, Brest, France; Ulrich Bleil, Institut für Geophysik, Ruhr-Universität, Bochum, Federal Republic of Germany; Peter E. Borella, Department of Oceanography, University of Washington, Seattle, Washington (now at: Riverside City College, Department of Physical Sciences, Riverside, California); Stefan Gartner, Department of Oceanography, Texas A & M University, College Station, Texas; Thierry Juteau, Université Louis Pasteur, Laboratorie de Minéralogie et Pétrographie, Strasbourg, France; Kerry Kelts, Swiss Institute of Technology, Geological Institute, Zurich, Switzerland (now at: Deep Sea Drilling Project, Scripps Institution of Oceanography, La Jolla, California); William N. Orr, University of Oregon, Department of Geology, Eugene, Oregon (now at: National Science Foundation, Ocean Sediment Coring Program, Washington, D.C.); Jean P. Quisefit, CNEXO, Boite Postale 337, 29273 Brest Cedex, France; Vladimir Rusinov, Institute of Geology, USSR Academy of Sciences; Moscow, USSR; Matthew Salisbury, Deep Sea Drilling Project, Scripps Institution of Oceanography, La Jolla, California; John M. Sinton, Department of Mineral Sciences, Smithsonian Institution, Washington, D.C. (now at: Hawaii Institute of Geophysics, University of Hawaii at Manoa, Honolulu, Hawaii); Brigitte M. Smith, Laboratoire de Géomagnetisme, St. Maur-des-Fosses, France; Stephan A. Swift, Department of Oceanography, University of Washington, Seattle, Washington (now at PMEL/DOMES, NOAA, Seattle, Washington); and Tadahide Ui, Department of Earth Sciences, Faculty of Science, Kobe University, Nada, Kobe, Japan.

Leg 52: Wilfred B. Bryan (Co-Chief Scientist), Woods Hole Oceanographic Institution, Woods Hole, Massachusetts; Paul T. Robinson (Co-Chief Scientist), Department of Earth Sciences, University of California, Riverside, California; Claire Bollinger, Centre Océanologique de Bretagne, Brest, France; Gary Byerly, National Museum of Natural History, Smithsonian Institution, Department of Mineral Sciences, Washington, D.C. (now at: Louisiana State University, Department of Geology, Baton Rouge, Louisiana); Rolf Emmermann, Institut für Petrographie und Geochemie der Universität-Karlsruhe, Karlsruhe, Federal Republic of Germany; Yozo Hamano, Geophysical Institute, University of Tokyo, Tokyo, Japan; Shaul Levi, Department of Geology and Geophysics, University of Minnesota, Minneapolis, Minnesota (now at: Oregon State University, School of Oceanography, Corvallis, Oregon); Gregory A. Miles, Department of Geology, University of Oregon, Eugene, Oregon (now at: Exxon Corporation, Exploration Department, Houston, Texas); Nikolai Pertsev, Institute of Ore Deposits and Geology, Moscow, USSR; Luc-Emmanuel Ricou, Laboratoire de Géologie Historique, Orsay, France; William G. Siesser, University of Cape Town, Rondebosch, South Africa; Ralph A. Stephen, University of Cambridge, Department of Geodesy and Geophysics, Cambridge, England (now at: Woods Hole Oceanographic Institution, Woods Hole, Massachusetts); Donald A. Swanson, U.S. Geological Survey, Menlo Park, California; and Stan White, Deep Sea Drilling Project, Scripps Institution of Oceanography, La Jolla, California.

Leg 53: Martin F. J. Flower (Co-Chief Scientist), Department of Geology, Imperial College, London, England (now at: Smithsonian Institution, National Museum of Natural History, Washington, D.C.); Matthew Salisbury (Co-Chief Scientist), Deep Sea Drilling Project, Scripps Institution of Oceanography, La Jolla, California; Dennis Bohrer, Deep Sea Drilling Project, Scripps Institution of Oceanography, La Jolla, California; Michael Hobart, Lamont-Doherty Geological Observatory, Palisades, New York; Douglas Johnson, Department of Geosciences, University of Texas at Dallas, Richardson, Texas (now at: University of Washington, Department of Geophysics, Seattle, Washington); Edmond Mathez, Department of Geological Sciences, University of Washington, Seattle, Washington; Catherine Mevel, Laboratoire de Pétrographie, Université Paris IV, Paris, France; Nikolai Pertsev, Institute of Ore Deposits and Geology, Moscow, USSR; R. G. Pritchard, School of Environmental Sciences, University of East Anglia, Norwich, England (now at: Department of Geology, University of Newcastle, Tyne and Wear, England); Harald Puchelt, Institut für Petrographie und Geochemie der Universität-Karlsruhe, Karlsruhe, Federal Republic of Germany; Peter A. Rigotti, Department of Geology, University of Pittsburgh, Pittsburgh, Pennsylvania (now at: Department of Geology and Geography, City University of New York, Hunter College, New York, New York); and Hubert Staudigel, Department of Earth and Planetary Sciences, Massachusetts Institute of Technology, Cambridge, Massachusetts (now at: Ruhr-Universität Bochum, Institut für Mineralogie, Bochum Federal Republic of Germany).

4) Does the petrology of Layer 2 evolve during construction and change with time? Layer 2A consists chiefly of mid-ocean ridge tholeiitic basalt showing evidence of extensive low-pressure crystal-liquid fractionation. Does Layer 2B consist of the same material, or can shallow magma chambers be maintained only after most of the crust has been formed? Are there systematic secular variations in the nature of mid-ocean ridge basalts as suggested by earlier studies, or have geochemical variations observed along the present Mid-Atlantic Ridge persisted through time?

5) What is the extent and nature of metamorphism in the oceanic crust? Measured heat-flow values near spreading ridges are generally much lower than theoretical values, suggesting the presence of large-scale hydrothermal circulation in the crust. However, little evidence of hydrothermal alteration or metamorphism has been found in the Layer 2A sections sampled thus far. This suggests that downwelling of cold sea water takes place over large areas but that upwelling of hot water is areally restricted. Has more extensive hydrothermal alteration occurred at depth or have the rocks been subjected to low-grade metamorphism? Is there a metamorphic gradient with depth in the crust and, if so, what chemical and mineralogical changes have occurred?

6) What is the nature and extent of sea-water alteration in the crust? Can the disappearance of Layer 2A in old crust be attributed to the infilling of voids and cracks by the products of alteration?

7) What is the source of linear sea-floor magnetic anomalies? Basement sections drilled thus far generally do not have sufficiently high magnetic intensities to account for the anomalies observed at the surface. Hence, the source of the anomalies must include the lower part of Layer 2 or the upper part of Layer 3. Do the anomalies reflect great thicknesses of low-intensity material or are they related to highly magnetic bodies as yet undiscovered? If the latter, what is the geometry of these bodies and how are they formed?

To study these problems, the Ocean Crust Panel of JOIDES recommended drilling a deep basement hole in old oceanic crust at the western end of the Atlantic Transect in the vicinity of the Bermuda Rise. The rationale for drilling in old crust was twofold. First, there was reason to believe that drilling would be easier because of infilling, thus increasing the chances for deep penetration; and second, by drilling old crust, we could study the effects of crustal aging. The Bermuda Rise was selected for the experiment since it lies on approximately the same flow line as the deep penetration holes drilled on Leg 45 (Melson, Rabinowitz, et al., 1979) and Leg 46 (Dmitriev, Heirtzler, et al., 1979) and because the basement is anomalously shallow for its age.

On the basis of these recommendations, a series of holes was drilled during Legs 51 through 53 in an area surveyed by R/V's *Lynch, Vema, Snellius, and Conrad* (Rabinowitz et al., this volume) at the southern end of the Bermuda Rise (Figure 1). The sites are located on or near anomaly *M*0 in 108- to 109-m.y.-old Cretaceous crust displaying low to moderate basement relief beneath a 200- to 300-meter-thick, gently undulating veneer of sediments. The Vema gap, which separates the Hatteras and Nares abyssal plains, lies in only slightly deeper water a few tens of kilometers to the southwest of the sites. The nearest fracture zones are 20 and 80 km to the northeast and southwest, respectively.

Although the sites drilled on Legs 51 through 53 were selected primarily to satisfy basement drilling objectives, several other considerations were taken into account:

The JOIDES Paleoenvironment Panel had noted that the Neogene section had only been spot-cored on previous legs in the Western Atlantic (Legs 1, 2, 4, 11, and 43). The Panel accordingly requested that the complete section be recovered on Legs 51 through 53 in order to examine the transition from siliceous, Pacific-type Eocene sedimentation to non-siliceous sedimentation resulting from the gradual emergence of the Central American isthmus.

Finally, we wished to examine in detail the thick Cretaceous-Tertiary section overlying the basement. At earlier sites drilled in the Western Atlantic (e.g., Sites 101, 386, and 387), the section had been found to consist predominantly of sublysocline, clay-rich sediments in the Tertiary and Upper Cretaceous which grade downward to more carbonate-rich Middle and Lower Cretaceous strata. Features of special interest at these sites included sedimentary hiatuses in the Paleogene and Upper Cretaceous sections, Paleogene and Upper Cretaceous clays with abundant zeolites and local metalliferous mineralization, and a variably organic "euxinic" Middle Cretaceous section. By drilling at the southern end of the Bermuda Rise, it was hoped to examine oceanic crust formed during a period when the Atlantic Ocean was euxinic to determine the consequences, if any, of the eruption of basaltic magmas into stagnant, organic muds. For example, would highly reduced alteration mineral suites be developed?

OPERATIONAL SUMMARIES

Leg 51

The *Glomar Challenger* left San Juan, Puerto Rico, on 20 November 1976, to drill a deep re-entry hole at Site 417. After a mudline core and washing test (Site 417), the ship was offset about 700 feet and redrilled a single-bit pilot hole (Hole 417A). The pilot hole was drilled in 5468 meters of water and penetrated 417 meters, of which 208 meters was in sediments and 209 meters in basaltic basement. The hole was continuously cored with a 60 per cent overall recovery, almost evenly divided between sediments and basalt. After the pilot hole was completed, the ship was offset another 450 meters; a re-entry cone was set, and multiple re-entry drilling begun at Hole 417D. A total of 533 meters was penetrated, of which 190 meters was in basaltic basement. The hole was logged (Salisbury et al., logging chapter, this volume) and left open for continued drilling on Leg 52. Two other holes (Holes 417B and 417C) were started and then abandoned in favor of the deep-penetration attempt in Hole 417D. The *Glomar*

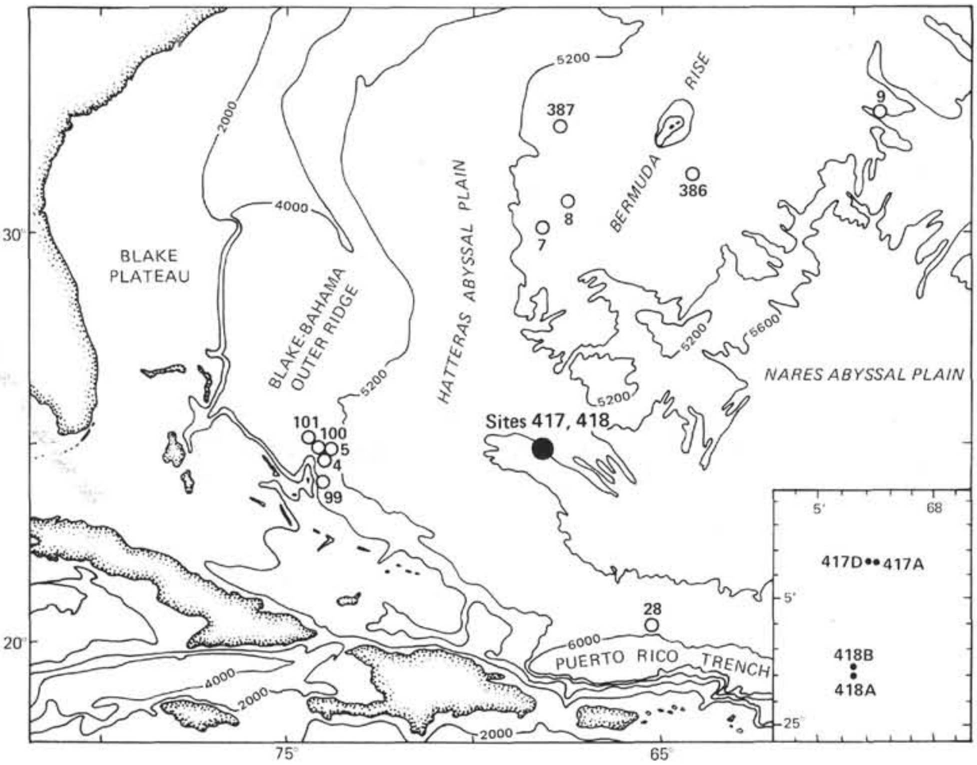

Figure 1. *Location of DSDP Holes 417A, 417D, 418A, and 418B. Oblique seismic and logging experiments were conducted in Hole 417D.*

Challenger returned to San Juan on 17 January 1977 upon completion of the Leg 51 phase of drilling.

Leg 52

The ship left San Juan for Site 417 on 22 January 1977, found and re-entered the hole begun on Leg 51 (Hole 417D), and continued drilling to a depth of 708.5 meters; at this point the hole had to be abandoned because of the loss of the bottom-hole assembly. Since the rate and ease of drilling at Site 417 and the extraordinarily high core recovery achieved on both Legs 51 and 52 indicated that the crust in the area was suitable for drilling, and the recovery of a nearly complete section through Layer 2 was technically feasible, we decided to make another attempt to drill a very deep hole at a second site (Site 418) about 4 nautical miles south-southwest of Site 417 at 25°02.08′N, 68°03.45′W (Figure 1). After taking a mudline core (Site 418), we set a second re-entry cone and drilled a new hole (Hole 418A) to a depth of 570.5 meters, of which 246.5 meters was in basalt. Toward the end of the leg, the ship returned to Hole 417D to rendezvous with the *Virginia Key* to conduct the oblique seismic experiment first attempted on Leg 46. After successfully completing the experiment (Stephen et al., this volume), Leg 52 was terminated in San Juan, Puerto Rico, on 8 March 1977.

Leg 53

The *Glomar Challenger* left San Juan on 12 March 1977 and returned to Site 418. The re-entry hole begun on Leg 52 (Hole 418A) was re-entered and deepened to 868 meters sub-bottom for a total basement penetration of 544 meters—45 meters short of the basement penetration record obtained on Leg 37 in Hole 332B (Aumento, Melson, et al., 1977). Drilling was terminated on 6 April 1977 owing to loss of the bottom-hole assembly. Although this assembly was subsequently recovered, the hole had to be abandoned when a logging tool became stuck in the hole. As in Hole 417D to the north, the basalt recovery in Hole 418A (72 per cent) was much higher than the sediment recovery (42 per cent). This was in part because cherts, jammed in the bit, often prevented sediments from entering the core barrel; and, more importantly, because voids and joints in the basalts had become sealed with smectite, calcite, and zeolites since their formation on the ridge crest, causing the rock to become mechanically homogeneous to drilling.

A final hole (Hole 418B) was drilled 130 meters to the north of Hole 418A in an attempt to recover portions of the sediment section not recovered during the drilling of Hole 418A on Leg 52. The hole was drilled to a depth of 329.6 meters of which 10 meters was in basalt. Although the hole was continuously cored, the objective was not completely fulfilled because of low core recovery (52 per cent). Leg 53 ended on 21 April 1977 at Balboa, The Canal Zone.

GEOLOGIC SUMMARIES

Site 417

The *Glomar Challenger* drilled two holes at Site 417: a pilot hole (Hole 417A) near the top of a small buried hill and a re-entry hole (Hole 417D) about 450 meters to the west near the base of the hill. The average basement slope between the holes was 16°.

The sediments recovered in the holes are similar to those found on previous Western Atlantic legs: nearly barren Tertiary clays (but with a radiolarian-rich middle Eocene section) resting on zeolitic, multicolored Upper Cretaceous clays with poorly preserved radiolarians, which in turn overlie green and black Middle Cretaceous claystones, highly burrowed nannofossil marls and chalks, and radiolarian sandstones (Figure 2). The black claystones are organic and contain pyrite, phosphates, and sphalerite. A thin, finely laminated chalk immediately above the basalt in Hole 417D yielded lower Aptian nannofossils, confirming the extrapolated age of anomaly *M*0.

The basalts drilled in Hole 417A consist of pillow lavas separated by green, smectite-rich hyaloclastic pillow breccias and thin massive basalts (Figure 2). The basalt is a rather uniform plagioclase-phyric rock with minor olivine and variable amounts of clinopyroxene, the latter commonly as extremely rounded phenocrysts. The massive basalts are fairly coarse grained and contain abundant plagioclase, clinopyroxene, and rare olivine pseudomorphs. The chemical composition of the basalt, as determined by shipboard X-ray fluorescence measurements, is fairly uniform, and represents typically plagioclase-rich mid-ocean-ridge basalt.

The basalts of Hole 417A show a degree of alteration far exceeding any seen in the Deep Sea Drilling Project. Even at a depth of 200 meters sub-basement, the basalts contain a rich variety of alteration minerals, including celadonite, smectite, K-feldspar, hematite, montmorillonite, calcite, and numerous zeolites.

The basalts drilled in Hole 417D consist almost entirely of porphyritic basalt and basalt breccia, with minor quantities of interlayered sediments in the upper part of the hole. Pillow basalts predominate, but interlayered massive units make up about 30 per cent of the section and generally become more abundant with depth. Broken pillow breccias are abundant in the interval between 605 and 642 meters sub-bottom and are present in small quantities at several other levels. Two dikes, each about 20 cm wide, occur in the lowest core. These are mineralogically and chemically similar to flows higher in the hole and may be feeder dikes.

The basalts in Hole 417D were divided into 14 stratigraphic units on the basis of variations in lithology and phenocryst assemblages (Figure 2). The units composed of pillow basalt range from 5 to 62 meters in thickness and commonly grade into broken pillow breccias. The pillow basalts are characterized by abundant glassy selvages, quench textures, and radial fractures. Spacing between glass rinds suggests a maximum pillow thickness of about 0.7 meter and an average thickness of about 0.45 meter. The stratigraphic units comprised of massive basalt flows range from about 5 to 25 meters in thickness. Single cooling units within these sequences are generally between 3 and 15 meters thick and characterized by a relatively coarse-grained matted groundmass. Glassy selvages are commonly present at the tops and bottoms of the units, and the grain size decreases toward the margins.

Nearly all of the basalts recovered in Hole 417D are porphyritic and contain 5 to 15 per cent phenocrysts. Three common phenocryst assemblages are present: plagioclase-olivine-clinopyroxene, plagioclase-olivine, and plagioclase alone; these occur in a crude stratigraphic sequence. The two basalt dikes at the bottom of the drilled section are both plagioclase-olivine-clinopyroxene-phyric. Chemically, the basalts show a narrow range of composition. Fresh samples have an average composition which is slightly fractionated compared to some ocean-ridge tholeiites but is similar to modern Mid-Atlantic Ridge basalts erupted at about the same latitude as Site 417. Downhole chemical variations correlate well with the stratigraphic sequence.

Considering their age (108 to 109 m.y.), the basalts in Hole 417D are remarkably fresh. A weathering zone 1 to 2 meters thick occurs at the top of the section but disappears rapidly downward, in marked contrast to the deep, pervasive weathering seen less than half a kilometer away in Hole 417A. Fresh glass persists in many selvages throughout the section (making this one of the few known instances of Cretaceous glass) and the crystalline basalts themselves also show little alteration. Olivine is the only phenocryst phase that is commonly altered. The most common secondary minerals are smectite, carbonate, pyrite, zeolite, and quartz. These often occur in vesicles, veins, and glassy selvages, but they also replace olivine and interstitial groundmass material in many basalts. Variations in alteration intensity correlate positively with the presence of fractures and breccias. The nature of the alteration and the observed secondary mineral assemblages indicate low-temperature interaction with sea water rather than hydrothermal alteration.

As noted above, the holes at Site 417 were drilled in crust corresponding to negative anomaly *M*0. Despite their alteration, the average NRM intensity of the samples from Hole 417A (8×10^{-3} emu/cm^3) is one of the highest ever recorded for either dredged or drilled basalts from the ocean crust, even from sites on the mid-ocean ridges. Furthermore, the average NRM inclination in the hole (−22°) is within 6° of that predicted for the site based on its latitude in the Cretaceous, suggesting that a 500-meter-thick basaltic layer with such properties would produce the observed *M*0 anomaly.

Hole 417D, however, is more complicated in that three distinct magnetic lithologies are observed in the basement section of the hole: (1)pillow lavas with negative NRM inclinations and a relatively high average magnetic intensity (1.4×10^{-2} emu/cm^3); (2) massive flows with positive NRM inclinations and low intensities (average 3.5×10^{-3} emu/cm^3); and (3) breccias with highly variable inclinations. The stable or cleaned inclinations in all of the rocks except a few breccias are negative in accord with the sense of the *M*0 anomaly. Stable inclinations are relatively uniform in the upper 148 meters of the section and average −65°. Below 148 meters the basalts have a mean stable inclination of

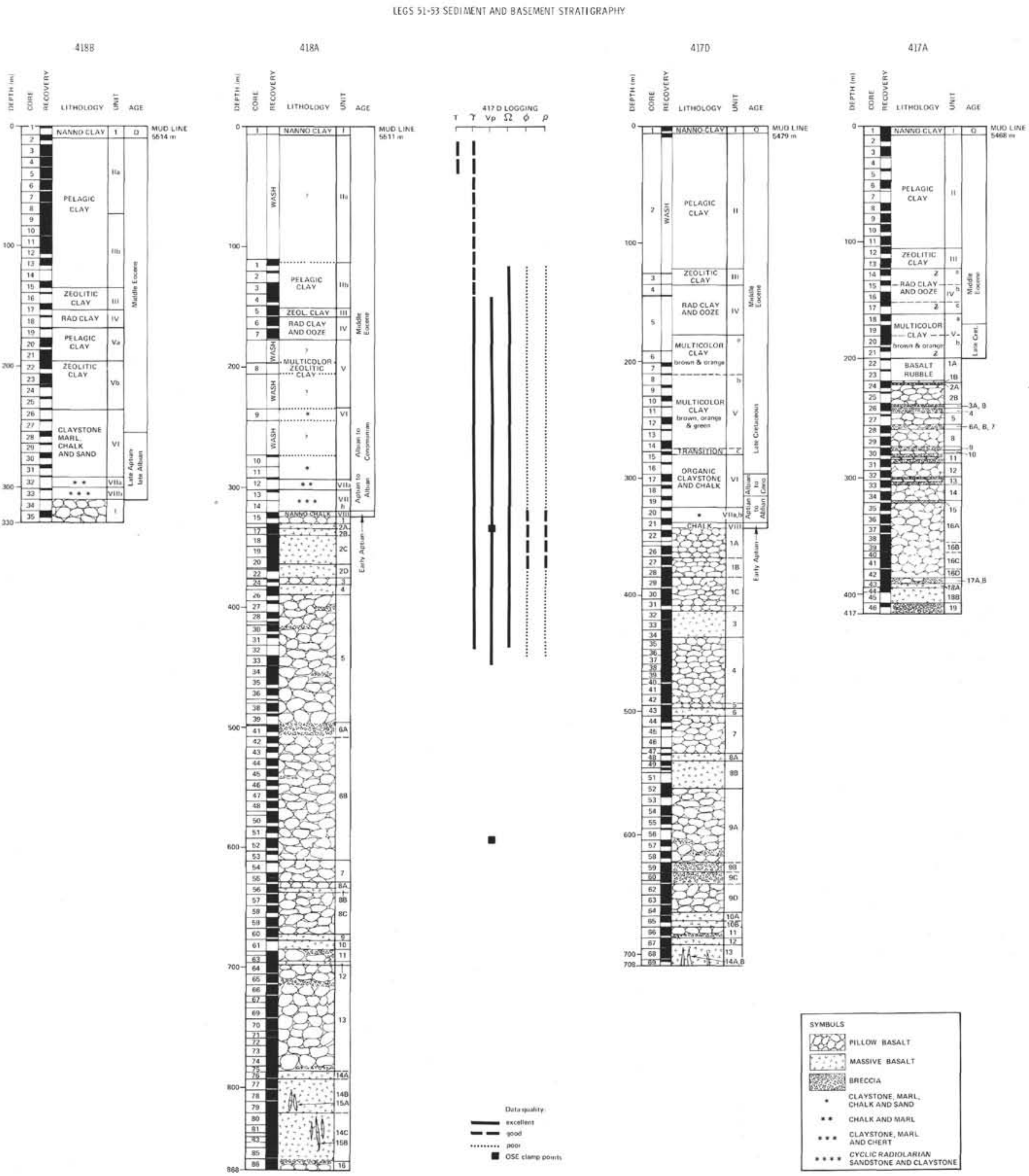

Figure 2. *Lithology versus depth in Holes 417A, 417D, 418A, and 418B. Also shown are estimates of the quality of the logging data and the positions of the geophone during the oblique seismic experiment in Hole 417D.* γ, V_p, Ω, ϕ, *and* ρ *stand for the natural gamma ray, velocity, resistivity, porosity, and density logs, respectively.*

$-27°$, which is almost identical to the predicted inclination for the site. However, in the lower part of the hole the inclinations systematically increase from $-18.8°$ at 302 meters sub-basement to about $-54°$ at 339 meters sub-basement, suggesting significant secular variation or tectonic rotation.

Measured sonic velocities (V_p) in the basalts at Site 417 range from 3.8 to 6.2 km/s and average about 5.5

km/s. The lowest values are from highly altered pillow lavas and pillow breccias, and the highest from fresh, massive flows. Wet-bulk densities range from 2.4 to 2.9 g/cm^3 and average 2.8 g/cm^3. Porosities range from a low of 2.6 per cent to over 25 per cent in some breccias. None of the basalts is highly vesicular, and the porosities probably result largely from fracturing and alteration. When compared with the results of downhole logging in Hole 417D and the oblique seismic experiment in the same hole, these data suggest that the upper levels of the crust at Site 417 are highly fractured *in situ* despite petrologic evidence of the partial sealing of the crust by the products of alteration. The results of the oblique seismic experiment also suggest that such cracks diminish with depth and become negligible near the boundary between Layers 2 and 3.

Site 418

Two holes were drilled at Site 418, a deep multiple reentry hole (Hole 418A) which achieved a total penetration of 868 meters (of which 544 m was in basement) and a single-bit hole (Hole 418B) designed to sample the sediment column. Both were drilled slightly to the east of anomaly *M*0 in a basement topographic depression analogous to that drilled in Hole 417D to the north.

In general, the sedimentary section at Site 418 is similar to that drilled at Site 417. The entire section, approximately 320 meters thick, consists of pelagic sediments, chiefly clays with minor nannofossil and radiolarian ooze (Figure 2). The section was divided into eight lithologic units on the basis of composition, mineralogy, and fossil content. The lower third of the section (Units VI to VIII) consist of interbedded dark gray, nonfossiliferous, pyrite-bearing clays and light blue, nannofossil-rich clay and clayey ooze, all of Cretaceous age (lower Aptian to lower Cenomanian). The upper two-thirds (Units I to V) consists chiefly of uniform brown to gray, pelagic clay with a layer of nannofossil clay at the top. Middle Eocene radiolarian clays occur in a thin interval in the middle of the section.

Fossiliferous zones are sparse in the cored section. An early Aptian age is derived for the sediments just above the basalt on the basis of diverse and moderately well preserved assemblage of nannofossils. Minor planktonic foraminifers and poorly preserved Cretaceous radiolarians are also present. The contact with the underlying basalt was not recovered but lies in the inferred age bracket for magnetic anomaly *M*0.

The basement section drilled in Hole 418A consists of 80 per cent pillow basalt and broken pillow breccia and 20 per cent massive basalt, the latter cut by high-angle dikes in the deepest levels of the hole. Minor calcareous sedimentary deposits occur between pillows throughout the section.

The basalts were divided into 16 stratigraphic units on the basis of morphology, lithology, and phenocryst assemblages (Figure 2). The stratigraphic units composed of pillow basalts and broken pillow breccias range in thickness from 7 to 113 meters. The pillows in these units have an average diameter of 0.5 meters and a maximum diameter of 1.1 meters. The massive basalt units, all of which are interpreted as flows, are most abundant at the top and bottom of the section and range in thickness from 2.7 to 73 meters. The thickness of individual cooling units, ranging between 2.1 and 38 meters, shows a rough cyclic variation with depth and appears to reflect a pattern of major eruptive episodes interspersed by lengthy quiescent intervals. Massive eruptions are less common than pillowed sequences and, in most cases, appear immediately or very shortly after major noneruptive periods inferred from breccia zones and magnetic breaks.

Most of the basalts recovered in Hole 418A are sparsely to moderately phyric and contain 5 to 10 per cent phenocrysts. Aphyric zones occur in some pillows, but these grade into phyric basalt over a distance of a few centimeters. Plagioclase is the dominant phenocryst, and is commonly six to eight times as abundant as olivine. Small olivine phenocrysts generally form less than 1 per cent of the rock, but locally form as much as 3 per cent. Clots or glomerocrysts of plagioclase and olivine are common, particularly in Unit 6. Clinopyroxene phenocrysts are much less abundant than in Hole 417D and occur in trace amounts only. Spinel is a minor but ubiquitous phase in Unit 6, where it forms red-brown to green-brown microphenocrysts or inclusions in plagioclase and olivine.

The groundmass of the pillow basalts is generally fine grained with glassy quench textures in which poorly crystallized clinopyroxene, intergrown with magnetite, forms plumose aggregates and radiating sheaves. The massive basalts in Hole 418A are more fine grained than those in Hole 417D and commonly display quenched, rather than mottled, textures.

As in Hole 417D, the basalts in Hole 418A are relatively fresh, particularly toward the base of the hole. The alteration in the upper levels of the hole is interpreted as being caused by low-temperature interaction of basalts with sea water. Smectite, carbonate, pyrite, zeolites, and silica are found in veins and vesicles, as the alteration products of glassy selvages or as replacement material in once-glassy detritus in broken-pillow breccia. Rarer alteration products such as orthoclase locally indicate more extreme alteration. Olivine and interstitial groundmass material are typically replaced by smectite and carbonate, but about half the olivine is fresh in the lower part of the hole. Plagioclase shows minor replacement along cleavage planes, usually by smectite. Glass occurs throughout the drilled section. Oxidation is more pronounced in the basalts from this hole than in those from the lower part of Hole 417D. It is localized along fractures and breccia zones and appears to postdate most of the alteration.

The chemistry of the basalts drilled in Hole 418A was studied by observing oxide variations among "fresh" rock analyses (i.e., corrected for carbonate contamination and with K_2O less than 0.2 weight per cent and H_2O^+ less than 1.25 weight per cent) normalized to dry weight, both within and between distinct eruptive cooling units. From this analysis, it was possible to define several distinct magma "batches" in the section each with a chemical or stratigraphic identity. These "batches" appear to fall within three main chemical groups:

(a) low TiO_2: TiO_2 = 1.0-1.15%; Mg/(Mg + Fe^{+2}) = 0.53-0.70; (b)moderate TiO_2; TiO_2 = 1.2-1.4%; Mg/(Mg + Fe^{+2}) = 0.54-0.66; (c) high TiO_2; TiO_2 = 1.5-1.7%; Mg/(Mg + Fe^{+2}) = 0.49-0.61.

Compositional differences between these types are probably due to fractional crystallization, accumulation of phenocrysts (especially plagioclase), various degrees of partial melting, magma mixing, or combination of these processes. All of the basalts are low-K tholeiites and nearly all are characterized by low to moderate TiO_2 contents. On a broader scale, perhaps the most significant observation is the difference in the range of TiO_2 and other oxides for equivalent MgO content and Mg/(Mg + Fe^{+2}) between fresh basalts cored in Cretaceous age crust in Holes 417D and 418A and those recovered at Sites 395 and 396 on Legs 45 and 46 in young crust to the west and east, respectively, of the Mid-Atlantic Ridge at 22°N.

On the basis of the magnetic profiles made by *Glomar Challenger*, the holes drilled at Site 418 are believed to have been drilled in positive anomaly crust just to the east of anomaly *M*0. Although the NRM and stable inclinations for the upper levels of the crust are positive (+24° in Hole 418A and +35° in the 10-m section drilled in Hole 418B), the magnetic stratigraphy for the crust as a whole is complex: the majority of the basalts in Hole 418A have a negative inclination, and at least five polarity reversals appear to have taken place during formation of the drilled section. As at several other sites in the Atlantic, we found intervals of steep NRM inclination (60 to 80°) inappropriate to the site's latitude. These anomalous inclinations are outside the range of normal secular variation and seem unlikely to be due to excursions of the Earth's field. In Hole 418A, dikes of normal polarity (+53.2 ±3.7°) traverse massive, reversely magnetized flows (-54.3 ±8.7°) in Unit 14 and have steep NRM inclinations almost identical to the inclination of the intruded lava sequence. The likelihood of this entire sequence having formed during an excursion is small, and we have interpreted this sequence as evidence for tectonic rotation of the deeper part of the eruptive pile before completion of the crustal section by later eruptions.

By equating magnetic reversals with unconformities and major NRM inclination changes with angular unconformities (rotation), nine major time breaks were identified within the Hole 418A section. Six of these correspond to breccia zones and five are marked by significant changes in basalt lithology. NRM intensities decrease with depth in the hole but for the most part are so high (the average intensity = 12.0 ±8.1 × 10^{-3} emu) that the strength of negative anomaly *M*0 can be completely accounted for by magnetization within Layer 2 alone.

The compressional wave velocities of the basalts in Hole 418A range from 4.0 to 6.3 km/s, while the densities range from 2.3 to 3.0 g/cm^3 and the porosities from 1 to 23 per cent. As at Site 417, the most altered basalts and breccias display the lowest velocities and densities and the highest porosities, while the massive basalts display the highest velocities and densities and the lowest porosities. Since the degree of alteration decreases with depth, the porosity of the basalt tends to decrease with depth while the velocity and density increase. A projection of the data versus depth suggests that the physical properties of the basalts approach the intrinsic values of fresh basalt at a depth of about 700 meters. This implies that only the upper half of Layer 2 has experienced significant alteration owing to interaction with sea water.

EXPLANATORY NOTES

Organization

The results of Legs 51, 52, and 53 are presented in two parts. In Part 1, the first section describes the background and objectives of the three legs and presents a brief summary of shipboard operations, a summary of the geologic results from all three legs, explanatory notes for the two volumes, and, finally, the detailed results of drilling at each site. The second section deals with geophysical surveys conducted in the area of the drill sites and with the results of special geophysical studies (downhole logging and the oblique seismic experiment) carried out in conjunction with the drilling program. The Appendices present grain size and carbon-carbonate analyses and data from the oblique seismic experiment.

Part 2 contains chapters that discuss extensively the results of shore-based investigations and data from the three legs. The final section of Part 2 presents synthesis chapters for the two volumes.

Authorship

In general, the material presented in the Site 417 chapter on Hole 417A was prepared by the Leg 51 shipboard party, while that shown for Hole 417D was prepared by the combined shipboard parties from Legs 51 and 52. Similarly, the material shown in the Site 418 chapter was largely prepared by the shipboard parties from Legs 52 and 53. In recognition of the innumerable instances of collaboration between scientists from all three legs, however, the authorship of the site chapters has been ascribed to the collective shipboard party from Legs 51, 52, and 53. Although most of the data shown in the site chapters were obtained on shipboard, the geochemical analyses include shore-based data obtained by H. Bougault, R. G. Pritchard, and H. Puchelt, and the biostratigraphic results were augmented by shore-based studies conducted by S. Gartner, R. Kozarek, and W. Orr.

Survey and Drilling Data

Survey data crucial to site selection and hole positioning are presented in the various site reports. While steaming between sites, continuous profiles of depth, total magnetic field, and sub-bottom seismic reflections were taken. Before dropping the beacon at each site, we made short surveys using a precision echo sounder, a seismic reflection profiler, and a proton precision magnetometer.

Underway depths were recorded continuously on an EDO-Western precision graphic recorder. The depths were read in meters, with an assumed sound velocity in water of 1500 meters/second. The sea-floor depth at each site was corrected for variations in sound velocity using the tables presented by Matthews (1939) and for the depth of the echo-sounder transducer (6 m). In addition, all depths referred to the drilling platform were calculated by assuming a distance of 10 meters between the floor of the drilling platform and the water line.

The seismic reflection profiling system consisted of two Bolt airguns, a Scripps-designed hydrophone array, Bolt amplifiers, two band-pass filters, and two EDO dry-paper recorders; the two recording systems normally operated at different scales and filter settings. Copies of the underway data may be obtained from Barbara Long at the Deep Sea Drilling Project, Scripps Institution of Oceanography, La Jolla, California.

Wide-angle reflection studies using free-floating SSQ-41A sonobuoys were conducted at Sites 417 and 418. The results are presented in the site reports under "Correlation of seismic reflection and drilling results." The methods and assumptions employed are also outlined in these reports.

Shipboard Procedures

Numbering Conventions and Core Handling Procedures

The drill sites are numbered consecutively from the first site drilled by the *Glomar Challenger* in 1968. The first (or only) hole drilled at a given site is assigned the site number; if more holes are drilled at the same site, the second is identified by the site number and the suffix A, the third by the site number and the suffix B, and so on.

The cores from each hole are numbered sequentially from the top down. In the ideal case (Figure 3), each core consists of 9.3 meters of sediment or rock in a plastic liner 6.6 cm in diameter. In addition, a 20-cm-long sample may be obtained from the core catcher (a multi-fingered device at the bottom of the core barrel that prevents cored material from sliding out of the core barrel while it is being brought to the surface). This sample represents the lowest material recovered in each core. The cored interval for each core is the interval in meters below the sea floor measured from the point at which coring was started to the point at which it was terminated. The interval is generally about 9.5 meters long (the nominal length of a core barrel), but may be shorter or longer depending upon the circumstances of drilling.

When a core and its enclosing liner are brought aboard the *Glomar Challenger*, they are cut into 1.5-meter sections, sealed, labeled, and moved into the core laboratory for processing. A full, 9.5-meter long core (including core catcher) consists of seven sections, numbered 1 through 7 from the top down. If less than

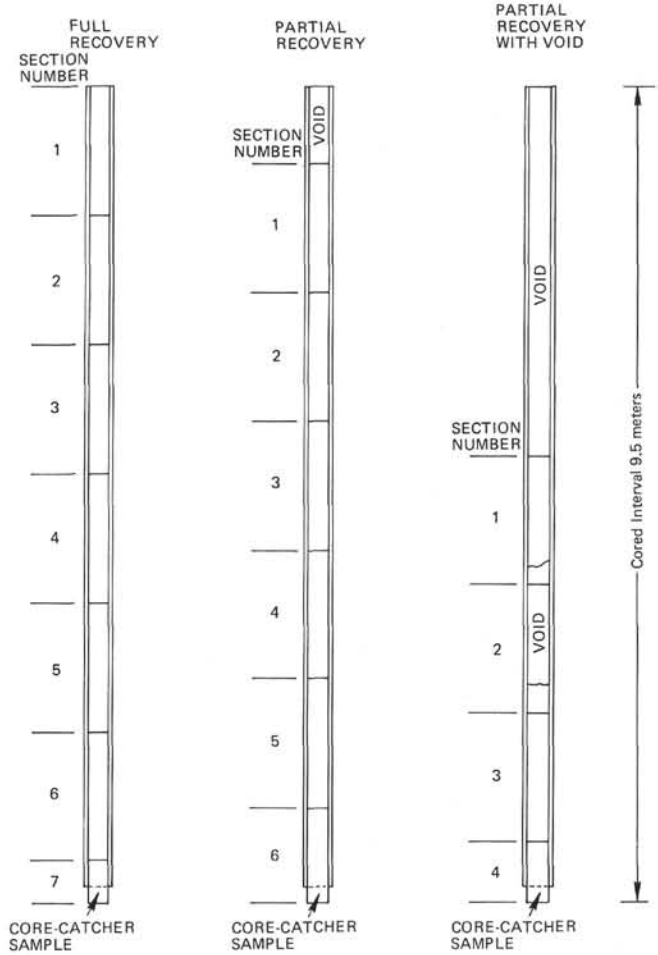

Figure 3. *Labeling of sections for various recovery configurations.*

9.5 meters is recovered, the sections are still numbered starting with 1 at the top but the number of sections is the number of 1.5-meter intervals needed to accommodate the length of core recovered. In such cases, the core recovery is measured from the top of the recovered material, with the top of Section 1 set equal to the top of the cored interval. Figure 3 illustrates the possible core configurations and the section-labeling procedure.

After an initial assessment of the age of the sediments in the core catcher and the wet-bulk density and porosity of the core have been determined by GRAPE (gamma ray attenuation) analysis, each 1.5-meter section is split longitudinally into an "archive" half and a "working" half. The former is photographed and described in terms of composition, color, texture, and structure as discussed below. The working half, after sampling for shipboard determination of grain size, carbon-carbonate, and water content, and for paleontology and physical property studies, is further sampled for subsequent shore-based analysis. Each sample taken from the core is designated by the interval, in centimeters, from the top of the section from which the sample was extracted; the sample volume, in cm^3, is also noted. Thus, a full sample designation would consist of the following information:

Leg (optional)
Site
Hole
Core Number
Section Number
Interval in centimeters from top of section
Sample size in cm^3

Thus, Sample 418A-1-3, 122-124 cm (10 cm^3) designates a 10-cm^3 sample taken from Section 3 of Core 1 from the second hole drilled at Site 418, Hole A. The depth below the sea floor for this sample would be the depth to the top of the cored interval plus 3 meters for Sections 1 and 2, plus 122 cm (depth below the top of Section 3), or 4.22 meters.

After the sediment cores are described and sampled, they are maintained in cold storage on the ship until transfer to the DSDP East Coast Repository (Lamont-Doherty Geological Observatory, Palisades, New York).

The handling of hard-rock material (e.g., basaltic rock) differs slightly from that of sediment cores. After the core has been cut into 1.5-meter-long sections and split with a rock saw into working and archive halves, the rocks are examined and thin styrofoam spacers are placed between those that cannot be fitted back together. The rocks are subdivided by this means into *pieces* which are numbered sequentially from the top of each section. If a piece consists of several fragments that fit together, these may be further identified by letter suffixes starting from the top of the piece (e.g., 8a, 8b, etc.). In practice, the spacers are used most often in basalt sequences to delineate intervals of no recovery or to indicate voids between pillows and in breccias. Since the thickness of the spacers is finite and arbitrary (about one-half centimeter), their insertion extends the apparent recovery. If, for any reason, it is necessary to determine the position of a sample in a core prior to the insertion of the spacers, the cumulative thickness of the spacers overlying the sample must be subtracted from its apparent depth.

After identification of each piece with a label indicating the hole, core, section piece, interval, and orientation (if unambiguous), the archive half is described, photographed, and placed in shrink tubing. The working half is then sampled for shipboard geochemical, magnetic, physical property, and thin-section studies and for subsequent shore-based analysis. After the cores have been described and sampled, they are maintained in cold storage on board until transfer to the DSDP East Coast Repository.

Shipboard Measurement Procedures

Physical Properties

A thorough discussion of the procedures used on shipboard to measure physical properties is given by Boyce (1973); we will offer only a brief review here.

1) The density and porosity of the samples recovered on Legs 51, 52, and 53 were measured by both gravimetric and gamma-ray attenuation (GRAPE) techniques. The gravimetric measurements were made on selected 2.54-cm-diameter minicores using the immersion method and a simple beam balance; after the wet-bulk density of each sample had been determined from its mass and volume, each sample was dried and reweighed in order to determine its porosity and grain density. Since the balance can be read to ± 0.01 g and the samples typically weigh about 30 g, the wet-bulk density measurements are considered accurate to better than 1 per cent. The porosity measurements are considered less accurate, owing to incomplete desiccation.

The GRAPE measurements were made on selected minicores by the 2-minute counting technique and on full sections of core by both the 2-minute and the continuous counting procedure (see Boyce, 1973). The method makes use of the Compton scattering of gamma ray by electrons in the sample to measure the electron density and thereby infer the bulk density of the sample. The gamma ray source used aboard the *Glomar Challenger* is ^{133}Ba, which emits gamma rays with energies of 0.300 MeV and 0.359 MeV. The gamma rays are scattered such that the beam intensity is given by the relation:

$$I = I_o e^{-\mu \rho_b dx}$$

where I is the measured beam intensity through the sample, I_o is the initial intensity (no sample), μ is the Compton mass attenuation coefficient (0.1024 cm^2/g for quartz), and ρ_b is the apparent bulk density of the sample. Thus one can obtain an approximate value for the bulk density of the sample from the relation,

$$\rho_b = \frac{\ln(I_o/I)}{\mu d},$$

where d is the sample thickness. The values obtained by this means were then corrected for variations in composition using the data from Müller (this volume). The porosity, ϕ, of each sample was finally determined from the relation,

$$\phi = \frac{\rho_g - \rho_b}{\rho_g - \rho_f},$$

where ρ_g is the average grain density of the sample and ρ_f is the density of the interstitial fluid (assumed to be 1.025 g/cm^3, the density of sea water). The porosity values obtained by these means were supplemented in the unconsolidated sediments at the top of each section by water-content determinations made by the syringe technique.

2) The compressional wave velocity of the samples was determined at atmospheric pressure using a Hamilton Frame velocimeter. The velocity is obtained by measuring the time of flight of a 400-kHz sonic pulse through a sample set between two transducers and measuring the thickness of the sample with a dial gage.

3) The shear strength of the sediments recovered on Legs 51, 52, and 53 was measured at room temperature and pressure using a Soiltest Torvane shear-strength meter with its axis of rotation aligned parallel to bedding. Since many of the samples measured had been disturbed during drilling, the values obtained can only be considered qualitatively correct.

4) The thermal conductivity of the sediments was measured to ± 4 per cent using the needle-probe technique described by von Herzen and Maxwell (1959). From three to five measurements were typically made 20 to 30 cm apart in each section examined. All measurements were made after the core had been allowed to equilibrate to room temperature.

5) The fluid permeability of a small number of basalt samples was determined by measuring the volume of fluid that passed through a sample of known cross-sectional area and thickness as a function of time after exposing one end to filtered sea water at a given pressure. The permeability was then calculated from the relation,

$$K = \frac{qud}{tpA}$$

where K is the fluid permeability of the sample in cm^2, q is the volume flux, u is the dynamic viscosity of the fluid, d is the sample thickness, t is the duration of the experiment, p is the pressure of the fluid, and A is the cross-sectional area of the sample.

Geochemical Measurements

The pH, alkalinity, chlorinity, salinity, and Ca^{++} and Mg^{++} contents of the recovered sediments are measured routinely on the ship.

1) The pH is determined by a flow-through electrode method in which a small portion of unfiltered water is passed through a glass capillary electrode.

2) The alkalinity is measured by colorimetric titration of a 1-ml aliquot of interstitial water with $0.1N$ HCl, using a Methyl Red/Blue indicator.

$$\text{Alkalinity (meq/kg)} = (\text{ml HCl titrated}) \cdot (97.752)$$

3) Salinity is calculated from the fluid refractive index as measured by a Goldberg optical refractometer, using the ratio,

$$\text{Salinity (‰)} = (0.55) \cdot \Delta N,$$

where ΔN = refractive index difference $\times 10^4$. Local surface sea water is regularly examined by each of the above methods to provide a reference for comparison.

Sedimentologic Analyses

1) Shipboard carbonate analyses were done by the "Karbonate Bombe" technique of Müller and Gastner (1971). In this procedure, a powdered sample is treated with HCl in a closed cylinder. The resulting CO_2 pressure is proportional to the amount of $CaCO_3$ in the sample. The technique is considered accurate to ± 2 to ± 5 per cent.

2) The shipboard carbon-carbonate data were determined using a LECO induction furnace combined with a LECO acid-base semi-automatic carbon determinator. Step-by-step procedures are presented in Volume 4 of the *Initial Reports of the Deep Sea Drilling Project,* and the methods, calibration, accuracy, and precision of the technique are discussed in Volume 9.

3) The grain-size distribution of the sediments was determined by standard sieve and pipette analysis. Step-by-step procedures appear in Volume 5 of the *Initial Reports.* In general, the sand-, silt-, and clay-sized fractions are reproducible to within ± 2.5 per cent (absolute). There is a discussion of this precision in Volume 9 of the *Initial Reports.*

Magnetic Measurements

The magnetic properties of the samples recovered on Legs 51, 52, and 53 were measured using a Digico balanced fluxgate magnetometer, a Schonstedt alternating field (AF) specimen demagnetizer, and a Schonstedt thermal demagnetizer. In addition, a number of samples on Leg 51 were studied using a susceptibility bridge.

The specimens examined were cut in the form of 1-inch cylindrical mini-cores aligned perpendicular to the drill string with an orientation arrow drawn on one face to indicate the vertical direction. This arrow is equivalent to the fiducial line referred to in the Digico manual, and points in the direction of the positive x-component of magnetization. The positive y-component is perpendicular to x in the plane of the flat face and is directed to the right, while the positive z-component is directed away from the flat face along the axis of the minicore. To restore the measured magnetic vector to its original orientation, a bedding correction in the Digico program is used to carry out a 90° rotation.

The magnetic properties determined on shipboard include measurements of the NRM intensity and inclination, stable inclination, initial susceptibility, and median demagnetizing field of the basalts and indurated sediments. A discussion of the procedures used is given in Levi et al. (this volume).

X-Ray Fluorescence Measurements

Whole-rock geochemical measurements were made during Legs 51, 52, and 53 using the CNEXO XRF van on the *Glomar Challenger.* The oxides analyzed were SiO_2, Al_2O_3, Fe_2O_3, MgO, CaO, TiO_2, K_2O, and P_2O_5. These analyses were supplemented by shipboard measurements of H_2O^+, H_2O^-, and CO_2 and by shore-based measurements of Na_2O, Cr, Ni, Sr, and Zr. The analytical techniques used to determine the major oxides were similar to those used on Leg 37 and discussed in detail by Bougault (1977).

X-Ray Diffraction Measurements

The bulk mineralogy of the sediments from all three legs was determined by shore-based X-ray diffraction studies conducted at Heidelberg University. The techniques used are discussed in detail by Biscaye (1965) and Müller (this volume).

Sediment Description Conventions

The sediments recovered are described on standard sediment description forms using the conventions discussed below and the symbols presented in Figures 4, 5, and 6:

Core Disturbance

Unconsolidated sediments are often severely disturbed during the rotary drilling/coring process and there is a complete gradation in the style of disturbance with increasing sediment induration. An assessment of the degree and style of drilling deformation is made onboard ship for all cored material and is shown graphically on the core description sheets. The following symbols are shown in Figure 4:

------ Slightly deformed; bedding contacts slightly bent.

— — — Moderately deformed; bedding contacts have undergone extreme bowing.

~~~~~~ Severely deformed; bedding completely disturbed, often showing symmetrical diapir-like structures, or water-saturated intervals that have lost all aspects of original bedding and sediment cohesiveness.

Smear Slides

The lithologic classification of sediments is based on visual estimates of the texture and composition in smear slides made onboard ship. These estimates are of areal abundances on the slide and may differ somewhat from the more accurate laboratory analysis of grain size, carbonate content, and mineralogy. Experience has shown that distinctive minor components can be accurately estimated to ±1 or 2 per cent, but that an accuracy of ±10 per cent for major constituents is rarely attained. The carbonate content is especially difficult to estimate in smear slides, as is the amount of clay present. The locations sampled for smear-slide analysis are given on the core description sheets.

Sediment Induration

The determination of induration is highly subjective, yet field geologists have successfully made such distinctions for many years. The criteria of Moberly and Heath (1971) are used for calcareous deposits; subjective estimates or behavior in core cutting are used for others.

a) Calcareous sediments
   - Soft: Oozes have little strength and are readily deformed under either the fine or the broad blade of a spatula.
   - Firm: Chalks are partly indurated oozes; they are friable limestones readily deformed under the fingernails or the edge of a spatula blade.
   - Hard: Cemented rocks are termed limestones.

b) The following criteria are used for other sediments:

   If the material is soft enough for the core to be split with a wire cutter, only the sediment name is used (e.g., silty clay; sand).

   If the core must be cut by a saw, the suffix "stone" is used (e.g., silty claystone; sandstone).

Color

Color is assigned according to standard Munsell or GSA color charts.

Sediment Classification

The sediment classification scheme used is basically that devised by the JOIDES Panel on Sedimentary Petrology and Physical Properties and adopted with minor modifications for use by the JOIDES Planning Committee in March 1974. The general classification scheme is outlined below. A compilation of the symbols used is given in Figures 5 and 6.

I. General rules for class limits and order of components in a sediment name.
   - A. Sediment assumes the names of those components present in quantities greater than 15 per cent.
   - B. Where more than one component is present, the component in greatest abundance is listed farthest to the right, and other components are listed progressively to the left in order of decreasing abundance.
   - C. The class limits are based on the percentage intervals given below for various sediment types.

II. Compositional Class Boundaries
   - A. $CaCO_3$ content (determined by $CaCO_3$ bomb) range between 30 and 60 per cent. With a 5 per cent precision and, given the natural frequency distribution of $CaCO_3$ contents in oceanic sediments, these boundaries can be reasonably ascertained.
   - B. Biogenic Opal Abundance
     Expressed as percentages of siliceous skeletal remains in smear slides: 10, 30, and 50 per cent. Smear slide estimates of identifiable siliceous skeletal material generally imply a significantly higher total opal abundance. The boundaries have been set to take this into account.
   - C. Abundance of Authigenic Components
     Zeolites, iron and manganese micronodules, fish bones, and other indicators of very slow sedimentation (estimated in smear slides); semiquantitative boundary: common 10 per cent. These components are conspicuous and a semiquantitative estimate is adequate. Because of the large difference in sedimentation rates, even a minor influx of calcareous, siliceous, or terrigenous material will dilute them to insignificance.
   - D. Abundance of Terrigenous Detrital Material
     Estimated from smear slides: 30 per cent.
~~~~~~

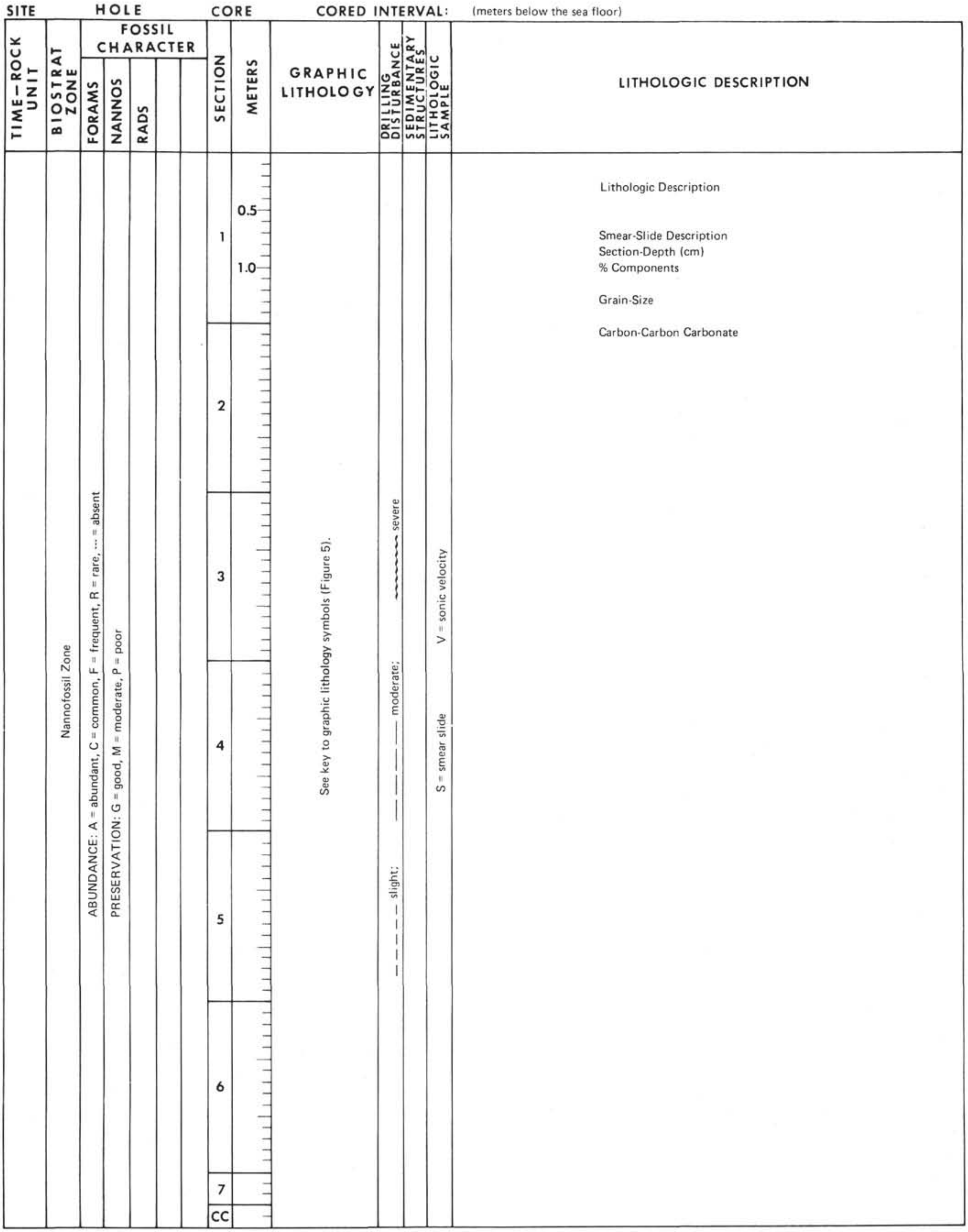

Figure 4. *Sediment description form.*

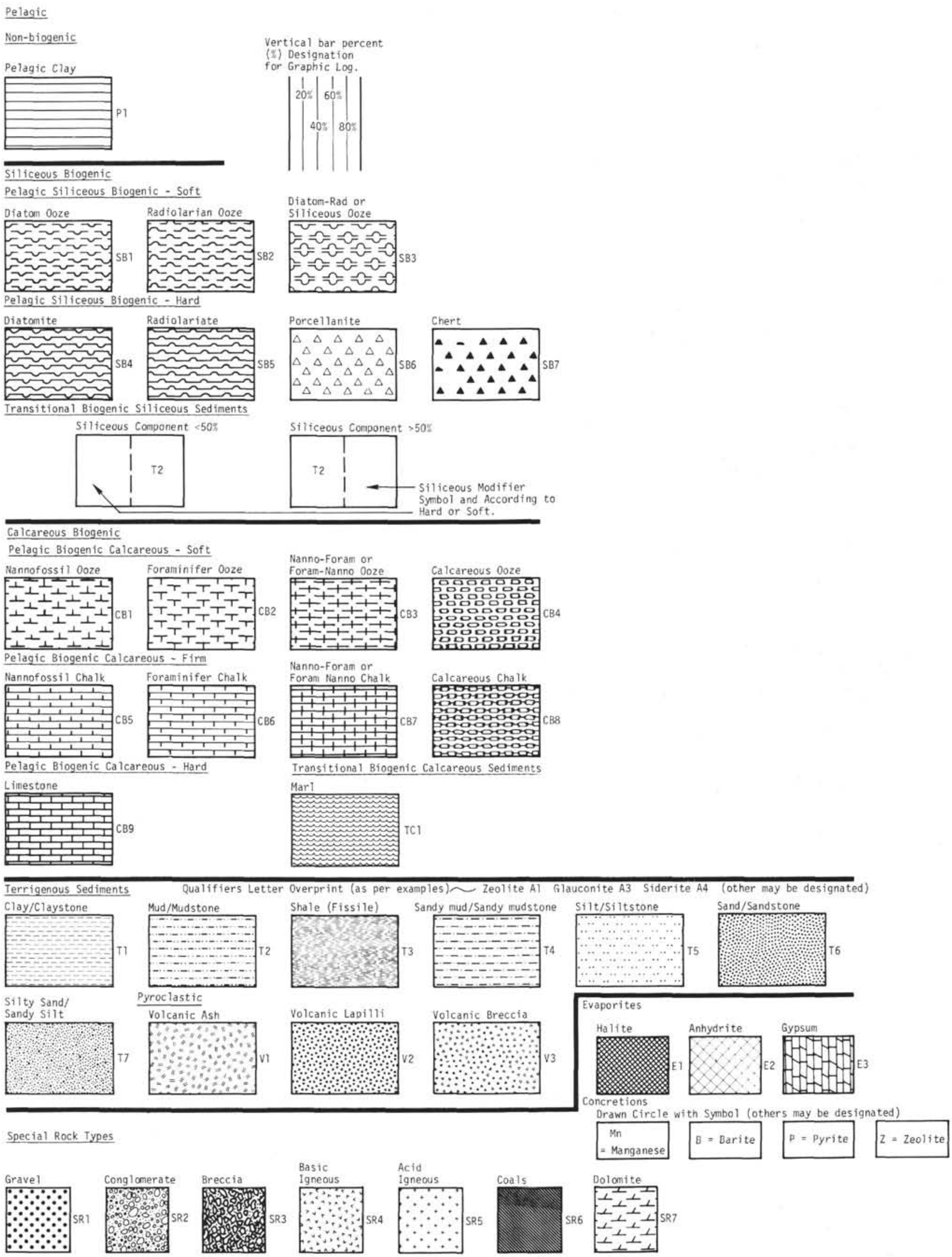

Figure 5. *Graphic symbols used in lithologic classification.*

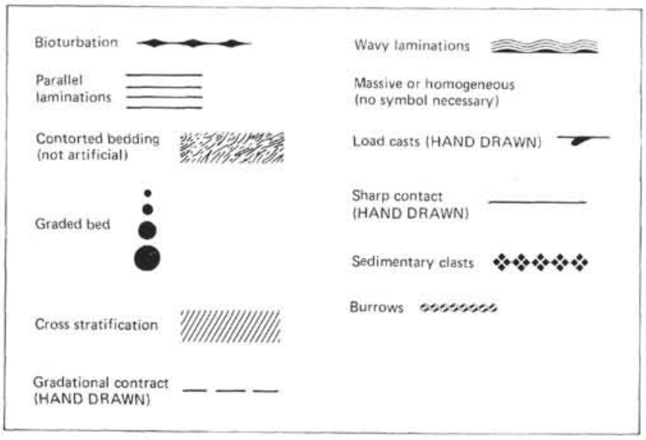

Figure 6. *Sedimentary structure symbols.*

E. Qualifiers
Numerous qualifiers are suggested; the options should be used freely. However, components of less than 5 per cent (in smear slide) should not be used as qualifiers except in special cases.

III. Description of Sediment Types (Figure 5)

A. Pelagic Clay
Principally authigenic pelagic deposits that accumulate at very slow rates. The class is often termed brown clay, or red clay, but since these terms are confusing, they are not recommended.

1. Boundary with Terrigenous Sediments
Where authigenic components (iron manganese micronodules, zeolites), fish debris, etc. become common in smear slides. NOTE: because of a large discrepancy in accumulation rates, transitional deposits are exceptional.
2. Boundary with Siliceous Biogenic Sediments
<30 per cent identifiable siliceous remains.
3. Boundary with Calcareous Biogenous Sediments
Generally, the sequence observed passes from pelagic clay through siliceous ooze to calcareous ooze. There is one important exception: at the base of many oceanic sections, black, brown, or red clays occur directly on basalt and are overlain by or grade upward into calcareous sediments. Most of the basalt clayey sediments are rich in iron, manganese, and metallic trace elements. For proper identification they require more elaborate geochemical work than can be done on shipboard. These sediments are placed in the "Special Rock" category, but care should be taken to distinguish them from ordinary pelagic clays.

B. Pelagic Siliceous Biogenic Sediments
These sediments are distinguished from the previous category for having more than 30 per cent identifiable siliceous microfossils. They are distinguished from the following category by a $CaCO_3$ content of less than 30 per cent. There are two classes: pelagic biogenic siliceous sediments (containing less than 30 per cent silt and clay); and transitional biogenic siliceous sediments (containing more than 30 per cent silt and clay and more than 10 per cent diatoms).

1. Pelagic Biogenic Siliceous Sediments
(a) Soft: Siliceous ooze (radiolarian ooze, diatom ooze, depending on dominant component).
(b) Hard: Radiolarite, porcellanite, diatomite, and chert.
(c) Qualifiers:
Radiolarians dominant — radiolarian ooze or radiolarite.
Diatoms dominant — diatom ooze or diatomite.
Where uncertain — siliceous (biogenic) ooze, chert or porcelanite; when containing >10 per cent $CaCO_3$, qualifiers are as follows:
Indeterminate carbonate: calcareous —
Nannofossils only: nannofossil —
Foraminifers only: foraminifer —
Nannofossil-foraminifer — / Foraminifer-nannofossil — : Depending on dominant component.
2. Transitional Biogenic Siliceous Sediments
Diatoms — <50 per cent diatomaceous mud: soft; diatomaceous mudstone: hard
Diatoms — >50 per cent muddy diatom ooze: soft; muddy diatomite: hard

Radiolarian equivalents in this category are rare and can be specifically described.

C. Pelagic Biogenic Calcareous Sediments
These sediments are distinguished from the previous categories by a $CaCO_3$ content in excess of 30 per cent. There are two classes: pelagic biogenic calcareous sediments (containing less than 30 per cent silt and clay); and transitional biogenic calcareous sediments (containing more than 30 per cent silt and clay).

1. Pelagic Biogenic Calcareous Sediments
(a) Soft: calcareous ooze
(b) Firm: chalk
(c) Hard: indurated chalk

The term limestone should be restricted to cemented rocks.

(d) Compositional Qualifiers:

Principal components are: nannofossils and foraminifers. One or two qualifiers may be used, for example:

Foram %	*Name*
<10	Nannofossil ooze, chalk, limestone
10-25	Foraminifer-nannofossil ooze
25-50	Nannofossil-foraminifer ooze
>50	Foraminifer ooze

Calcareous sediments containing more than 10 to 20 per cent identifiable siliceous fossils carry the qualifier radiolarian, diatomaceous, or siliceous, depending on the quality of the identification; for example: radiolarian-foraminifer ooze.

2. Transitional Biogenic Calcareous Sediments
   (a) $CaCO_3$ 30 to 60 per cent: Marly calcareous pelagic sediments.
   Soft: Marly calcareous (or nannofossil, foraminifer, etc.), ooze (see below).
   Firm: Marly chalk.
   Hard: Marly limestone.
   (b) $CaCO_3$ >60 per cent: calcareous pelagic sediments
   Soft: Calcareous (or nannofossil, foraminifer, etc.) ooze (see below).
   Firm: Chalk
   Hard: Limestone

NOTE: Sediments containing 10 to 30 per cent $CaCO_3$ fall into other classes, where they are denoted with the adjective "calcareous." If the $CaCO_3$ content is under 10 per cent, it is ignored.

D. Terrigenous and Volcanogenic Sediments
1. Terrigenous Sediments
Sediments falling within this category are subdivided into textural groups on the basis of the relative proportions of clay, silt, and sand. Rocks coarser than sand size are treated as "Special Rock Types." The size limits for these constituents are those defined by Wentworth (1922). Five major textural groups are recognized. They are defined according to the abundance of clay (>90 per cent, 90 to 10 per cent, and <10 per cent) and the ratio of sand to silt (>1 or <1). Sands and sandstones may be subdivided further into very fine-, fine-, medium-, coarse-, and very coarse-grained categories according to their median grain size.
(a) Qualifiers
In this group numerous qualifiers are possible, usually based on minor constituents; for example: glauconitic, pyritic, feldspathic. In the sand and sandstone category, conventional divisions such as arkose and graywacke are, of course, acceptable, providing the scheme is properly identified. Clays, muds, silts, and sands containing 10 to 30 per cent $CaCO_3$ are called calcareous.
2. Volcanogenic Sediments
Pyroclastic rocks are described according to the textural and compositional scheme of Wentworth and Williams (1932). The textural groups are:

Volcanic breccia fragments	>32 mm
Volcanic lapilli fragments	<32 mm
Volcanic ash (tuff, if indurated) particles	<4 mm

The compositions of pyroclastic rocks are described as vitric (glass), crystalline or lithic.
3. Clastic Sediments of Volcanic Origin
These sediments are described in the same fashion as terrigenous sediments, with the dominant composition of the volcanic grains noted where possible.

E . Special Rock Types
The definition and nomenclature of rock types not included in the system described above are left to the discretion of shipboard scientists, with the recommendation that they adhere as closely as possible to conventional terminology.
In this category fall such rocks as:
Intrusive and extrusive igneous rocks (see below)
Evaporites (halite, anhydrite, gypsum, etc.)
Shallow-water limestone (biostromal, biohermal, coquina, and oolite)
Dolomite
Gravels, conglomerates, breccias.

Biostratigraphic Conventions

The scope of paleontological and biostratigraphic studies for Legs 51 through 53 is limited due mainly to a lack of recovery of fossiliferous sediment. The bulk of the sediment cored was a pelagic clay or zeolitic clay which is virtually barren of fossil remains. Fossiliferous sediments were recovered, however, over selected intervals. Calcareous fossils were recovered from a near-surface calcareous layer in Holes 417, 417B, 417D, 418, and 418B. The calcareous nannofossil and planktonic foraminifers in this layer contain a mixture of late Pliocene and Pleistocene elements. Very probably these calcareous sediments were displaced by a turbidity current from a shallower depth. Age assignments for this calcareous layer are based on comparison of the flora/fauna within the layer, with the biostratigraphic succession set down in various calcareous nannofossil and planktonic foraminiferal zonations. No exotic or novel interpretation of the evidence was made. Calcareous fossils were also recovered from sediments near basement at Holes 417D, 418A, and 418B. These near-basement calcareous sediments are associated with black, sapropelic clays characteristic of Early and "mid"-Cretaceous sedimentation in the eastern North Atlantic Basin. Calcareous nannofossil ages are based largely on the zonation of Thierstein (1971, 1973, 1976); Sissingh (1977); and Roth and Thierstein (1972). Planktonic foraminiferal ages are based on the zonation compiled by van Hinte (1976).

Siliceous microfossils, chiefly radiolarians, were recovered from Holes 417A, 417D, 418A, and 418B. Consistent occurrence of radiolarians is associated with middle Eocene sediments at these sites, the level corresponding with the widespread episode of deposition of siliceous ooze in the North Atlantic. Radiolarians also occur in Upper Cretaceous pelagic clays, although these are far less abundant than the middle Eocene forms, and are always very poorly preserved. More abundant radiolarians were encountered in the Cretaceous sediments near the base of the sediment section at Holes 417A, 417D, and 418B, although frequently the remains at this level consist of little more than casts and molds. Radiolarian age determinations are based largely on the published works of Riedel (see e.g., Riedel and Sanfillipo, 1978) for the Cenozoic, and on the successions documented by Pessagno for the Mesozoic (Pessagno, 1976).

Fish teeth were also recovered in small numbers in residues from the sieving of large amounts of otherwise barren clay. Though sparse, these remains were useful in a general way for biostratigraphic subdivision of otherwise barren intervals. Age assignments are based largely on the succession of ichthyoliths elaborated by Doyle and Riedel (in preparation).

Basement Description Conventions

Core Forms

The core description forms (Figure 7) used for igneous and metamorphic rocks are not the same as those used for sediments. Each form covers one 1.5-meter section in order to provide space (if needed) for piece-by-piece hand specimen descriptions as well as thin-section, chemical, and physical property data. The left-hand box on the form is for a visual representation of the working half of the core. In addition, two closely spaced horizontal lines are drawn in this column wherever a styrofoam spacer has been placed to separate unrelated pieces. All orientable pieces are indicated by an upward-pointing arrow to the right of the graphic representation. The locations of samples taken for shipboard studies are indicated in the "Shipboard Studies" column using the following notation:

X = X-ray fluorescence and CHN chemical analysis
M = magnetic measurements
S = sonic velocity measurements
T = thin section
D = density measurements
P = porosity measurements

The state of alteration (see Figure 7 for symbols) is shown in the column labeled "Alteration." On Legs 51 through 53 some pieces were stored permanently in salt water. These are labeled with a "W" in the "Special Storage" column.

Igneous Rock Classification

The igneous rocks drilled on Legs 51, 52, and 53 were classified mainly on the basis of mineralogy and texture. Thin-section work in general added little new information to the hand-specimen classification.

Basalts are termed aphyric, sparsely phyric, moderately phyric, or phyric, depending on the proportion of phenocrysts visible with the binocular microscope ($\sim \times 12$). The basalts are called aphyric if phenocrysts are absent. For practical purposes, this means that if one piece of basalt is found with a phenocryst or two in a section where all other pieces lack phenocrysts, and no other criteria such as grain size or texture distinguish this basalt from the others, then it is described as aphyric. A note on the rare phenocrysts is included in the general description, however. This approach enables us to restrict the number of lithologic units to those that appear to be clearly distinct.

Sparsely phyric basalts are those with 1 to 2 per cent phenocrysts present in almost every piece of a given core or section. Clearly contiguous pieces without phenocrysts are included in this category, again with the lack of phenocrysts noted in the general description.

Moderately phyric basalts contain 2 to 10 per cent phenocrysts. Aphyric basalts within a group of moderately phyric basalts are separately termed aphyric basalts.

Phyric basalts contain more than 10 per cent phenocrysts. No separate designation is made for basalts with more than 20 per cent phenocrysts; the proportion indicated in the core forms should be sufficient to guide the reader.

The basalts are further classified by phenocryst type, preceding the terms phyric, sparsely phyric, etc. For example, a plagioclase-olivine moderately phyric basalt contains 2 to 10 per cent phenocrysts, most of them plagioclase, but with some olivine.

REFERENCES

Aumento, F., Melson, W. G., et al., 1977. *Initial Reports of the Deep Sea Drilling Project*, v. 37: Washington (U. S. Government Printing Office).

Biscaye, P. E., 1965. Mineralogy and sedimentation of recent deep sea clay in the Atlantic Ocean and adjacent seas and oceans, *Geol. Soc. Am. Bull.*, v. 76, p. 803-832.

Bougault, H., 1977. Major elements, analytical chemistry on board and preliminary result. *In* Aumento, F., Melson,

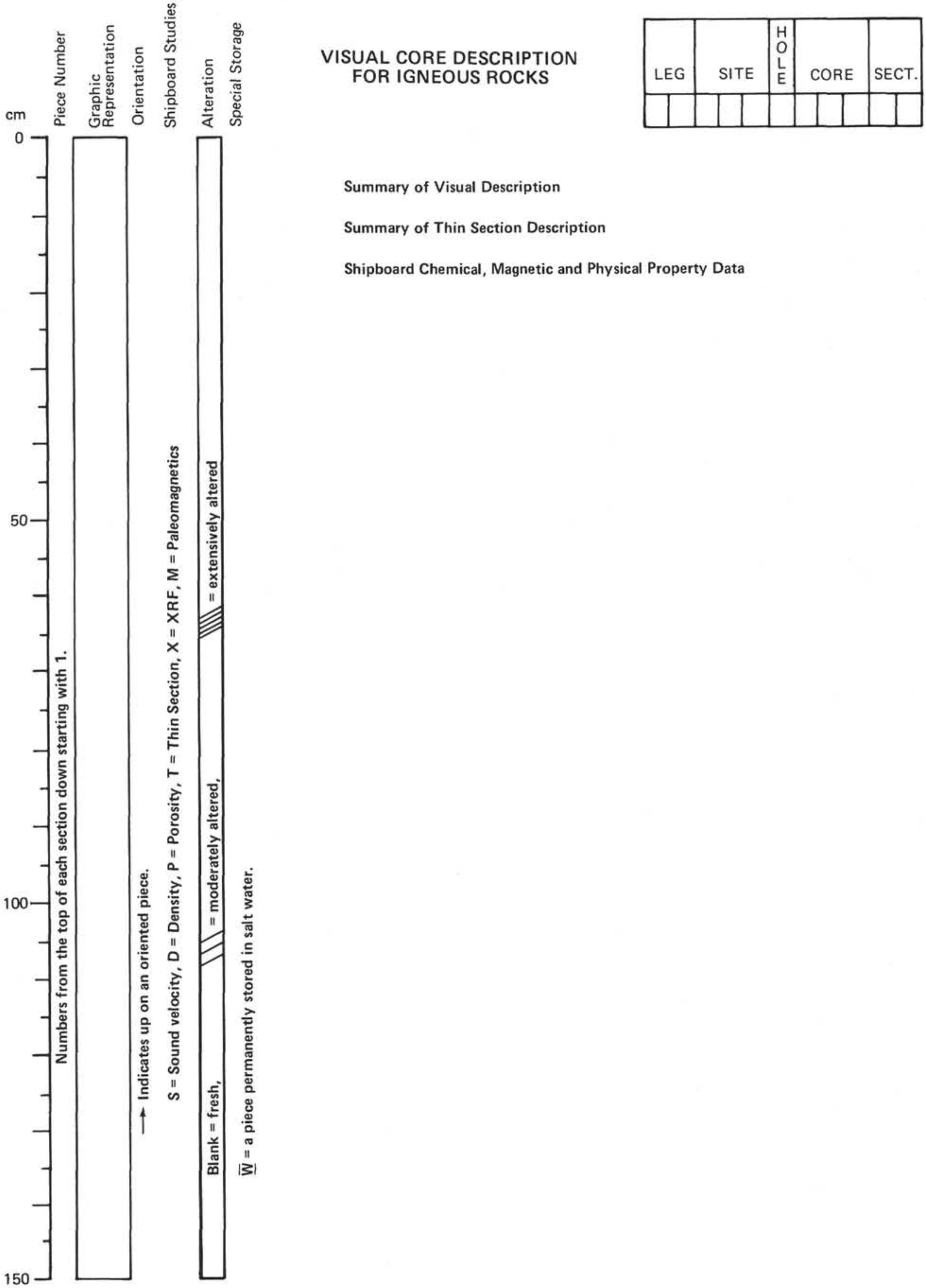

Figure 7. *Description form for igneous rocks.*

W.G., et al., *Initial Reports of the Deep Sea Drilling Project*, v. 37: Washington (U. S. Government Printing Office), p. 643-657.

Boyce, R. E., 1973. Physical properties — methods. *In* Edgar, N. T., Saunders, J. B., et al., *Initial Reports of the Deep Sea Drilling Project*, v. 15: Washington (U. S. Government Printing Office), p. 1115-1127.

Cann, J. R., Luyendyk, B., et al., 1979. *Initial Reports of the Deep Sea Drilling Project*, v. 49: Washington (U. S. Government Printing Office).

Dmitriev, L., Heirtzler, J., et al., 1978. *Initial Reports of the Deep Sea Drilling Project*, v. 46: Washington (U. S. Government Printing Office).

Doyle, P. S. and Riedel, W. R., in preparation. Cretaceous to Neogene ichthyoliths in a giant piston core from the central North Pacific.

Matthews, T., 1939. *Tables of the Velocity of Sound in Pure Water and Sea Water for Use in Echo Sounding and Sound Ranging:* London (Admiralty Hydrographic Department).

Melson, W. G., Rabinowitz, P. D. et al., 1979. *Initial Reports of the Deep Sea Drilling Project*, v. 45: Washington (U. S. Government Printing Office).

Moberly, R., Jr., and Heath, G. R., 1971. Carbonate sedimentary rocks from the western Pacific: Leg 7, Deep Sea Drilling Project. *In* Winterer, E. L., Riedel, W. R., et al., *Initial Reports of the Deep Sea Drilling Project*, v. 7, Part 2: Washington (U. S. Government Printing Office), p. 977-985.

Müller, G. and Gastner, M., 1971. The "Carbonate Bomb," a simple device for the determination of the carbonate content in sediments, soils, and other materials, *N. Jb. Mineral.*, v. 10, p. 466-469.

Pessagno, E. A., 1976. Radiolarian zonation and stratigraphy of the Upper Cretaceous portion of the Great Valley sequence, California Coast Ranges, *Micropaleontology*, Spec. Publ. 2, p. 1-87.

Riedel, W. R. and Sanfillipo, A., 1978. Stratigraphy and evolution of tropical Cenozoic radiolarians, *Micropaleontology*, v. 23, p. 61-96.

Roth, P. H. and Thierstein, H., 1972. Calcareous nannoplankton: Leg 14 of the Deep Sea Drilling Project. *In* Hayes, D. E., Pimm, A. C. et al., *Initial Reports of the Deep Sea Drilling Project*, v. 14: Washington (U. S. Government Printing Office), p. 421-485.

Sissingh, N., 1977. Biostratigraphy of Cretaceous calcareous nannoplankton, *Geologie en Mijnbouw*. v. 56, 1, p. 37-65.

Thierstein, H. R., 1971. Tentative lower Cretaceous nannoplankton zonation, *Eclog. Geol. Helv.*, v. 64, p. 459-488.

________, 1973. Lower Cretaceous calcareous nannoplankton biostratigraphy, *Abhandlungen der Geologischen Bundesanstalt*, v. 29, p. 1-52.

________, 1976. Mesozoic calcareous nannoplankton biostratigraphy of marine sediments, *Marine Micropaleontology*, v. 1, p. 325-362.

van Hinte, J. E., 1976. A Cretaceous time scale, *Am. Assoc. Petrol. Geol. Bull.*, v. 60, p. 498-516.

von Herzen, R. and Maxwell, A. E., 1959. The measurement of thermal conductivity of deep-sea sediments by a needle-probe method, *J. Geophys. Res.*, v. 46, p. 1557.

Wentworth, C. K., 1922. A scale of grade and class terms of clastic sediments, *J. Geol.*, v. 30, p. 377.

Wentworth, C. K. and Williams, H., 1932. The classification and terminology of the pyroclastic rocks, *Rept. Comm. Sed., Nat. Res. Council, Bull.*, no. 89, p. 19-53.